

Detection of individual trees and estimation of tree height using LiDAR data

Doo-Ahn Kwak · Woo-Kyun Lee · Jun-Hak Lee ·
Greg S. Biging · Peng Gong

Received: 11 May 2007 / Accepted: 30 August 2007 / Published online: 19 October 2007
© The Japanese Forest Society and Springer 2007

Abstract For estimation of tree parameters at the single-tree level using light detection and ranging (LiDAR), detection and delineation of individual trees is an important starting point. This paper presents an approach for delineating individual trees and estimating tree heights using LiDAR in coniferous (*Pinus koraiensis*, *Larix leptolepis*) and deciduous (*Quercus* spp.) forests in South Korea. To detect tree tops, the extended maxima transformation of morphological image-analysis methods was applied to the digital canopy model (DCM). In order to monitor spurious local maxima in the DCM, which cause false tree tops, different h values in the extended maxima transformation were explored. For delineation of individual trees, watershed segmentation was applied to the distance-transformed image from the detected tree tops. The tree heights were extracted using the maximum value within the segmented crown boundary. Thereafter, individual tree data estimated by LiDAR were compared to the field measurement data under five categories (correct delineation, satisfied delineation, merged tree, split tree, and not found). In our study, *P. koraiensis*, *L. leptolepis*, and *Quercus* spp. had the best detection accuracies of 68.1% at $h = 0.18$, 86.7% at $h = 0.12$, and 67.4% at $h = 0.02$, respectively. The coefficients of determination for tree height estimation were 0.77, 0.80, and 0.74 for *P. koraiensis*, *L. leptolepis*, and *Quercus* spp., respectively.

Keywords Individual trees · LiDAR · Morphological image analysis · Tree height · Tree top

Introduction

Forest inventory information has been important with respect to forest management. In addition, for sustainable forest management, more information is needed, not only for planning future forest management, but also for recording the previous status of the forested area (Koch et al. 2006). Furthermore, single-tree-level forest information has been essential for various forest applications, such as monitoring forest regeneration, forest inventory, and evaluating forest damage (Chen et al. 2006). Therefore, detailed forest information, such as tree counts, tree heights, crown base heights, diameter at breast height (DBH), and forest biomass, are critical for the effective management and quantitative analysis of forests. However, the traditional methods of investigating such parameters involve labor-intensive forest inventories, the incorporation of complex sampling designs, and supplementary work (Avery and Burkhart 1994; Shivers and Borders 1996). Moreover, the existing methods are time-consuming, subjective, and more applicable to small areas (Avery and Burkhart 1994). Therefore, over the last few years, new technologies, like remote sensing, have supplemented and supplanted some of these field measurements. Although different types of sensor have been used to extract forest information, light detection and ranging (LiDAR), especially, has recently been used to extract surface information, as it can acquire highly accurate object shape characteristics using geo-registered 3D points (Kwak et al. 2006). Therefore, the LiDAR system can measure both vertical and horizontal forest structures in forested areas,

D.-A. Kwak · W.-K. Lee (✉)
Division of Environmental Science and Ecological Engineering,
Korea University, Seoul 136-701, South Korea
e-mail: leewk@korea.ac.kr

J.-H. Lee · G. S. Biging · P. Gong
Division of Environmental Science, Policy and Management,
University of California at Berkeley, Berkeley, CA 94720, USA

such as tree heights, sub-canopy topographies, and distributions, with high precision (Holmgren et al. 2003). Such characteristics measured using LiDAR can also be applied for modeling of the above-ground biomass, stem counts and crown widths (Dubayah and Drake 2000; Lefsky et al. 2002) as they can typically be used to automatically generate the digital canopy model (DCM), which can describe the outer contour of the tree crowns (Holmgren and Persson 2004). Even though several papers have shown that large-footprint LiDAR is a good means for estimating tree parameters, with an averaging and stand-wise approach (Næsset 1997; Lefsky et al. 1999; Maltamo et al. 2006), stand-wise forest information is insufficient for detailed forest management planning, such as thinning, harvesting, and planting trees, or for quantifying forest volume, biomass, and carbon absorption ability. Therefore, extracting single-tree-level information using small footprint LiDAR is necessary in many cases where such detailed field work is required (Koch et al. 2006).

To obtain single-tree information from remotely sensed data, regardless of aerial photographs, satellite imagery, or LiDAR, it is essential to detect and delineate individual trees. Early attempts at the detection and delineation of individual trees using remotely sensed data were carried out with multispectral imagery (Koch et al. 2006). To delineate individual trees using such imagery, several methods have been applied, including the valley-following method (Gougeon 1995), multiple scale edge segmentation (Brandtberg and Walter 1998), template matching (Pollock 1996), watershed segmentation (Scharadt et al. 2002), and local maxima filtering (Dralle and Rudemo 1996). However, when delineating individual trees using previously established methods with imagery, the crowns at least need to be visually recognizable as discrete objects. Therefore, recognition of crowns requires the spatial resolution of the imagery to be higher than the size of the crowns. Imagery with relatively low spatial resolution is not applicable for identification and delineation of individual trees. In addition, it was assumed the delineation of tree crowns could be accomplished using imagery, since the center of a crown (peak) in the image is brighter than the edge (valley) (Wulder et al. 2003). However, the difference in the reflectance value between the center and edge of the crown is not always distinct, due to influencing factors such as the crown spectral property, complicated crown texture, diverse forest structure, and time of imagery acquisition (Wulder et al. 2003).

For resolving such difficulty, LiDAR remote sensing technology has recently been applied to the delineation of individual trees and for the extraction of canopy information (Hyypä et al. 2001; Persson et al. 2002; Chen et al. 2006), because LiDAR data can actively acquire tree crown and canopy information using geo-registered 3D-points,

which are difficult to obtain by direct use of passive sensors. Once the DCM has been created from the LiDAR data, the individual trees can be delineated and their heights estimated, because the DCM contains a geometrical elevation according to the peaks and valleys of a canopy. Some papers have applied similar methods to LiDAR, but used aerial photographs or satellite imagery. Leckie et al. (2003) applied the valley-following method whereas Brandtberg et al. (2003) carried out crown segmentation by using multiple scale edge segmentation. Persson et al. (2002) attempted tree delineation using local maxima detection, and Mei and Durrieu (2004) segmented tree crowns using watershed segmentation with LiDAR data. However, in these cases, the accuracy of delineating individual trees was relatively low, due to the broad variation of height in the DCM as a result of detailed LiDAR information. Although such simple smoothing methods could reduce the depth of pits and small peaks through smoothing, it could not remove commission or omission errors, so over-segment problems still can occur (Chen et al. 2006). Thus, to decrease these errors, Popescu and Wynne (2004) accomplished tree segmentation using the local maxima detecting method by adopting flexible window sizes according to the relationship between the tree height and crown size. As another method for improving the accuracy of delineated individual trees, Chen et al. (2006) presented marker-controlled watershed segmentation, which performs watershed segmentation around user-specified markers in the input image, rather than the local maxima, to remove false tree tops.

The objectives of this paper were to:

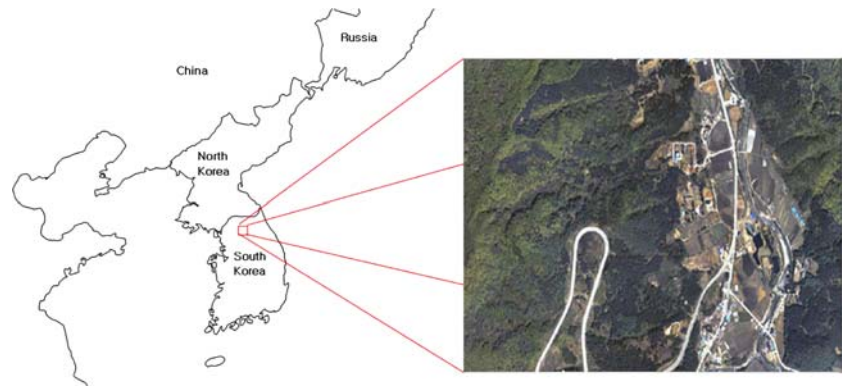
1. optimally detect tree tops and delineate individual trees according to species (*Pinus koraiensis*, *Larix leptolepis*, and *Quercus* spp.), using the extended maxima transformation and the distance transformation of the morphological image-analysis methods; and
2. estimate individual tree heights from the delineated single trees.

If both objectives are successful, the LiDAR data can be considered for modeling various tree parameters, such as crown base heights, diameter at the breast height, basal areas, tree volumes, and the aboveground biomass, in the forested areas of South Korea.

Methods

Study area

The study area was located on Mt Yumyeong (upper left 127°29'0.19380"E, 37°36'16.43433"N and lower right 127°30'1.10"E, 37°35'42.94"N), central South Korea (Fig. 1).

Fig. 1 The study area

Approximately 80 ha of private forests were selected for this study. Situated from 321 to 573 m above sea level, the study area was dominated by steep hills, with the main tree species being *P. koraiensis* (Korean Pine), *L. leptolepis* (Japanese Larch), and *Quercus* spp. (Oaks). These stands were selected in such a way that the composition of tree species was homogeneous, but the edges of the individual tree crowns were very closely overlapped with each other due to the high tree density.

LiDAR and ground data

In this study, Optech ALTM 3070 (a small footprint LiDAR system) was used for acquisition of the LiDAR data, with the flight performed on 28 April 2004. The study area was measured from an altitude of 1,500 m, with a sampling density of 1.8 points per square meter, and the radiometric resolution, scan frequency, and scan width were 12 bits, 70 Hz, and $\pm 25^\circ$, respectively. The information of all objects was derived from the first and last returns. The sample sites were composed of 15 plots, each with an area of 100 m² (10 m \times 10 m), with five plots per tree species. For all plots, 135 trees, *P. koraiensis* (47), *L. leptolepis* (45), and *Quercus* spp. (43), were measured for their individual tree heights and positions. The positions of the individual trees were acquired at the breast height of the individual trees, using GPS Pathfinder Pro XR manufactured by Trimble. Ground data were obtained on 16 October 2004, although the LiDAR data were acquired on 28 April 2004. However, the difference in the tree height growth relevant to the period between the acquisition of the ground data and LiDAR-derived values was not considered, as tree height growth during 6 months is relatively small, on the basis of the tree height growth rate calculation (Table 1).

Classification of LiDAR data and derivation of DCM

In order to derive the DCM from the LiDAR data, pre-classified points were used with the TerraScan software

(Terrasolid Corporation, Jyväskylä, Finland); therefore, raw LiDAR points were classified into one of four groups: ground return (GR), low vegetation return (LVR), medium vegetation return (MVR), and high vegetation return (HVR) (Lim et al. 2001). The DCM was computed by subtracting the digital terrain model (DTM), as a representation of the ground area, from the digital surface model (DSM), as a representation of the surface of the crowns. The DSM and DTM were generated with the TIN (triangulated irregular networks)_{HVR} and TIN_{GR} from the HVR and GR points, respectively. All the work for generating the DCM, DTM, and DSM was carried out using ESRI's ArcGIS 9.0. As not all the HVR points represented the outermost surface, the use of all the HVR points for generating TIN produces an incorrect spurious surface model. Especially, the across-track distances between points were relatively further than the along-track distance; therefore, the surface model could have false strips in the flying direction (Fig. 2a). In order to cope with this problem, the HVR and GR were filtered with a 1 m \times 1 m window to select only the highest and lowest points within the window, with these filtered points used to generate the DSM and DTM (Fig. 2b).

Segmentation of individual trees

Extended maxima process for detecting tree tops

The watershed transformation is a powerful partitioning tool for a gray-scale image. Due to the similarity between the DSM and gray-scale images, the watershed transformation is also useful for delineating single trees from the DSM (Chen et al. 2006). The watershed segmentation method can find the edges (valleys) of each crown in the DCM, and the top (peak) of individual trees can be extracted within each crown boundary. However, general watershed segmentation methods have problems in that the number of individual trees may be overestimated or underestimated due to the large height variation within

Table 1 Descriptive statistics of the field measurements

Species	Number of trees	Height (m)			
		Minimum	Maximum	Mean	SD
<i>Pinus koraiensis</i>	47	10.8	20.2	15.6	2.3
<i>Larix leptolepis</i>	45	11.0	23.5	16.4	2.7
<i>Quercus</i> spp.	43	8.5	18.8	14.2	2.5

their topography or smaller tree tops under the crowns of the higher trees. For successful delineation, selecting a suitable marker and input function are important (Dougherty and Lotufo 2003). In our study, tree tops were detected for marker and transformation functions, which changed the original DSM into another image, to delineate the crown boundaries. Consequently, individual trees were segmented after finding the tree tops using the extended maxima transformation and distance transformation of the morphological image-analysis methods, which removed the problem of over-segmentation found with normal watershed segmentation. If these methods are applied to the DCM, smaller pseudo tree tops on the crown topography are removed using the user-specified value (h value) of the extended maxima transformation.

The extended maxima transformation is the regional maxima transformation of the H-maxima transformation, as shown in Eq. (1) (Soille 2003).

$$\text{EMAX}_h(f) = \text{RMAX}[\text{HMAX}_h(f)]. \quad (1)$$

As the first step in the extended maxima transformation, a set of all H-maxima transformations is denoted by HMAX. The HMAX transformation suppresses all maxima whose depth is lower than or equal to a given threshold level, h , which is achieved by performing a reconstruction by dilation of f from $f - h$:

$$\text{HMAX}_h(f) = R_f^\delta(f - h), \quad (2)$$

where f is an input image, h a nonnegative scalar, R a reconstruction function, and δ a dilation operator. In this study, f is the DCM and $R_f^\delta(f - h)$ is defined as the geodesic dilation of f with respect to $f - h$, and iterated until stability is reached (Soille 2003). The geodesic dilation of f with respect to $f - h$ performs the morphological dilation for $f - h$, but the value of f is applied only in the case where the value after the dilation for $f - h$ is greater than f (Fig. 3). In the DCM, the h value of the HMAX transformation can play a key role as a factor for controlling the segmentation level, such as over or under estimation of the number of individual trees, by removing unnecessary maxima according to tree species. Because the shapes according to tree species will be different, the DCM has different height variations and tree species shapes. Therefore, a reasonable result for delineating individual trees by controlling the h value according to the tree species can be obtained. In this paper, the optimal h value was estimated in 0.02 steps, from 0.00 to 0.30, for tree delineation according to tree species.

In the second step, a regional maxima transformation is required to find the tree tops of f_{hmax} treated by the H-maxima transformation. The set of all regional maxima transformations is denoted by RMAX, and defined by the threshold superposition, as shown in Eq. (3) (Soille 2003).

$$\text{RMAX}(f_{\text{hmax}}) = f_{\text{hmax}} - R_{f_{\text{hmax}}}^\delta(f_{\text{hmax}} - 1), \quad (3)$$

where f_{hmax} is the image after H-minima transformation with the DCM, and $R_{f_{\text{hmax}}}^\delta(f_{\text{hmax}} - 1)$ is defined as the geodesic dilation of f_{hmax} with respect to $f_{\text{hmax}} - 1$, iterated until stability is accomplished, as in the HMAX process. However, the detection of maxima using reconstruction in RMAX subtracts $R_{f_{\text{hmax}}}^\delta(f_{\text{hmax}} - 1)$ from f_{hmax} . Therefore, a binary image, which has a value of 1 can be obtained, corresponding to a tree top of the f_{hmax} belonging to the regional maxima, otherwise 0 is used if the RMAX

Fig. 2 DCM generated with all points (a) and DCM generated with filtered points (b)

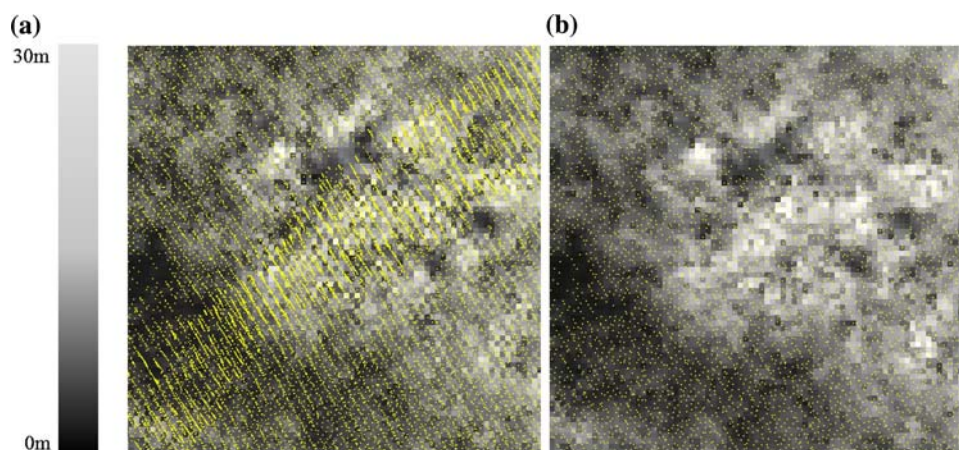
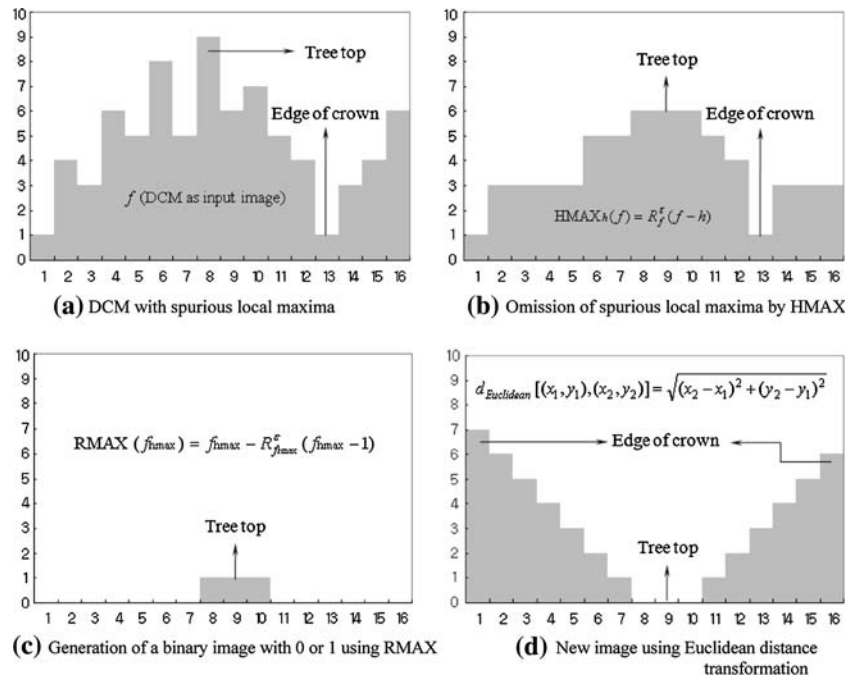


Fig. 3 Process of segmenting individual trees



transformation is carried out with the $f_{h_{max}}$ after the HMAX transformation (Fig. 3).

Segmentation of individual trees

For segmenting individual trees, the $f_{DT(E_{max})}$ was generated after treatment of the Euclidean distance transformation with the $f_{E_{max}}$ generated using the extended maxima transformation. The Euclidean distance transformation is defined by assigning a number that is the distance between that value and the nearest nonzero value of the black and white image (Soille 2003). The Euclidean distance between (x_1, y_1) and (x_2, y_2) in the black and white image ($f_{E_{max}}$) created using the extended maxima transformation is expressed, as shown in Eq. (4).

$$d_{Euclidean}[(x_1, y_1), (x_2, y_2)] = \sqrt{(x_2 - x_1)^2 + (y_2 - y_1)^2}, \tag{4}$$

where (x_i, y_i) are the coordinates of a pixel on $f_{E_{max}}$. In the process of Euclidean distance transformation, a value of 1 s, tree tops in a binary image, is transformed into 0 s, otherwise values of 0 s in a black and white image are converted into the distance from the neighboring value of 1 s (Fig. 3). Therefore, values of 0 s in $f_{DT(E_{max})}$ are real tree tops, with the relatively highest values among the neighbors being valleys of a real canopy between tree tops. Thus, the tree crown boundaries can be directly obtained using a distance transformation with $f_{E_{max}}$.

Estimation of tree heights

After the segmentation, the individual tree heights are estimated using $f_{DT(E_{max})}$ and the DCM. When estimating tree heights, individual trees delineated with a one-to-one relationship were used. Individual tree heights were determined from the highest elevation value of the DCM within the segmented boundaries. The tree height (h) is the maximum value within the segmented polygon

$$h = \max (h_i), \tag{5}$$

where h_i is the individual tree height of the corresponding segment polygons (Hyypää et al. 2001).

Accuracy analysis

Using the $f_{DT(E_{max})}$ generated from different h values, according to tree species, the accuracy of individual tree detection can be evaluated. To evaluate the accuracy of individual tree detection, field measurements were carried out according to tree species in each 10 m × 10 m area. In comparison with the field data, each segmented tree was visually classified into one of the five categories suggested by Leckie et al. (2003), as shown in Table 2. However in this study, satisfactory delineation refers to a segmented boundary that was visually slightly larger or smaller than the reference tree crown, whereas in the work of Leckie et al. (2003) this meant the areas of both trees overlapped by less than 60%.

Additionally, the estimated tree heights were compared with the field measurement data, as an accuracy assessment, using the coefficient of determination (R^2) and root mean square error (RMSE).

Results

Segmentation of individual trees

The accuracy of detected individual trees was estimated using the five categories in Table 2, according to the h values from the extended maxima transformation for the three tree species. To evaluate the accuracy of detection, the individual trees, classified into the correct and satisfactory categories in Table 2, were assumed to have a one-to-one relationship with field-measured trees. The segmentation accuracies according to the different h values, at 0.02 intervals, were estimated and are depicted in Fig. 4. With increasing h values, the segmentation accuracies also increased and reached their highest value, after which the accuracies started to decrease.

The best detection accuracies for *P. koraiensis*, *L. leptolepis*, and *Quercus* spp. were 68.1% at $h = 0.18$, 86.7% at $h = 0.12$, and 67.4% at $h = 0.02$, respectively. In similar studies, the accuracy of tree detection had a broad range values. Leckie et al. (2003), who used the same accuracy assessment method as in this study, detected individual trees with a 59% match for a coniferous forest. Koch et al. (2006), with the same assessment method, found trees with an 87.3% match for Douglas firs (*Pseudotsuga menziesii*) and 50% for deciduous trees (*Carpinus betulus*, *Acer pseudoplatanus* and *Fraxinus excelsior*). In the study of Chen et al. (2006), 64.1% of trees were detected with the method, with one-to-one corresponding trees at the ground truth crown boundary for Blue oaks (*Quercus douglasii*). The accuracies in this study appear to be similar to those of other research. However, it is difficult to conclude which research should be recommended for detecting trees in forest areas, as each of these studies used specific algorithms for segmentation, and different accuracy assessment methods and study areas.

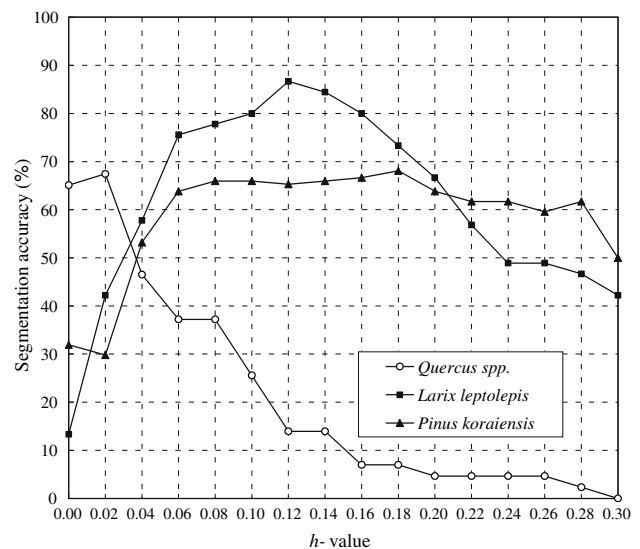


Fig. 4 Accuracies for correct and satisfactory segmentation according to h values and tree species

It was noticeable that *Quercus* spp. had a narrow fit range, with an accuracy of over 60%, which abruptly decreased with increasing h value, while other coniferous trees had relatively wide fit ranges (Fig. 4). The h values with accuracies of over 60% ranged from 0.06 to 0.20, 0.06 to 0.28, and 0.00 to 0.02 for *L. leptolepis*, *P. koraiensis* and *Quercus* spp., respectively. This can be attributed to the tree form differences between coniferous and deciduous tree species. When h is very large for deciduous trees, the tree crowns can have under-segmentation (merged), as the tree tops required for segmentation are removed. For *Quercus* spp., the merged rates reached 77 and 86% at $h = 0.12$ and 0.18 , respectively, whereas *L. leptolepis* and *P. koraiensis* had the best segmentations. The merged rate for *Quercus* spp. decreased to 23% at $h = 0.02$ (Table 3).

In contrast, if h is very small for coniferous trees, the tree crowns can be over-segmented (split) due to several spurious local maxima, which are counted as initial points for segmentation. At $h = 0.02$, where *Quercus* spp. reached the best accuracy, 64% of *P. koraiensis* and 51% of *L. leptolepis* were over-segmented or split. This over-

Table 2 Categories for accuracy analysis in tree crown segmentation

Categories	Definition
Correct delineation	Exactly 1:1 correspondence between reference tree and detected tree
Satisfactory delineation	One automatically detected tree corresponds to one reference tree, but the boundaries are larger or smaller than the reference tree crown
Merged tree	More than one reference tree lies within the automatically delineated tree
Split tree	More than one automatically-delineated tree lies within one reference tree
Not found	There exists a reference tree, but no corresponding automatically delineated tree

segmented (split) rate decreased to 17% at $h = 0.18$ for *P. koraiensis* and 13% at $h = 0.12$ for *L. leptolepis*.

Pinus koraiensis had the best detection at $h = 0.18$ (shown bold in Table 3), and the rates of split and merged trees occupied 17.02 and 14.89%, respectively. In the case of *L. leptolepis*, the best detection was accomplished at $h = 0.12$, with 13.33% split trees, and without merged trees. The best detection for *Quercus* spp. was reached at $h = 0.02$, and the rates of split and merged trees were 23.26 and 4.65%, respectively. The most appropriate h values for different tree species can be found by applying various h values, and then analyzing the segmentation result.

Figure 5 depicts the segmented image according to the h value with the highest accuracy. Circles refer to the positions of individual trees obtained through the field survey, and the “x” marks are the tree tops detected through the extended maxima transformation with LiDAR data. The positions and tree tops of individual trees fell within the segmented crown polygon, but some spatial differences were found between the field and LiDAR positions.

Estimation of tree height

The tree heights estimated from 100 crowns (32 *P. koraiensis*, 39 *L. leptolepis*, and 29 *Quercus* spp.), delineated with the correct and satisfactory categories in Table 2, were compared to field measurements. The coefficients of determination for tree height estimations were 0.77, 0.80, and 0.74 for *P. koraiensis*, *L. leptolepis* and *Quercus* spp., respectively (Fig. 6), while Clark et al. (2004) estimated the height in a tropical rain forest with a coefficient of determination of 0.51. The RMSEs were 1.13, 1.35, and 1.32 m for *P. koraiensis*, *L. leptolepis*, and *Quercus* spp., respectively. In this study, the accuracy of the heights of the coniferous trees was usually higher than for the deciduous trees, which was similar to that found by Heurich et al. (2004), but they estimated the accuracy at 0.96

for coniferous trees and 0.98 for deciduous trees. However, this cannot be directly compared due to the different forest types, densities, compositions of tree species, and quality of the LiDAR data.

Discussion

Our research showed that coniferous trees were better segmented, with relatively higher h values than deciduous trees. A coniferous crown has a cone shape, with a steep slope, so there are definite differences in the elevation values among pixels on the DCM from the tree top to the crown edge. It can allow the top and bottom of the crown to be easily found. However, small conical swellings can exist on the crown surface of a coniferous tree, causing an individual tree to be segmented into several trees. This can generate spurious tree tops, which are the initial point of segmentation. Therefore, when coniferous trees are delineated using the extended maxima transformation and distance transformation, as in this paper, a higher h value must be selected to remove unnecessary swellings. On the other hand, deciduous trees have an ellipsoidal crown shape, which has a gentle slope, so there are slight differences in the elevation values among pixels in the DCM. In comparison to coniferous trees, difficulty can be encountered in finding the top and bottom of the crown with deciduous trees. The swellings on a deciduous crown are rarely recognized compared to those on a coniferous crown. Therefore, a lower h value can be employed for removing relatively rounded swellings when segmenting deciduous trees. These different h values for coniferous and deciduous trees can imply that different h values should apply to different forest types for detecting individual trees. To find optimal h values for different forest types and tree species, further research is needed with various types of forests and trees.

Table 3 Segmentation results with optimal h values according to tree species

h value	Tree species	Total	Correct		Satisfactory		Merged		Split		Not detected	
			Number	%	Number	%	Number	%	Number	%	Number	%
0.18	<i>Pinus koraiensis</i>	47	25	53.19	7	14.89	7	14.89	8	17.02	0	0.00
	<i>Larix leptolepis</i>	45	28	62.22	5	11.11	4	8.89	5	11.11	3	6.67
	<i>Quercus</i> spp.	43	1	2.33	2	4.65	37	86.05	1	2.33	2	4.65
0.12	<i>Pinus koraiensis</i>	47	22	44.90	10	20.41	4	8.16	11	26.53	0	0.00
	<i>Larix leptolepis</i>	45	34	75.56	5	11.11	0	0.00	6	13.33	0	0.00
	<i>Quercus</i> spp.	43	4	9.30	2	4.65	33	76.74	1	2.33	3	6.98
0.02	<i>Pinus koraiensis</i>	47	7	14.89	7	14.89	0	0.00	30	63.83	3	6.38
	<i>Larix leptolepis</i>	45	8	17.78	11	24.44	0	0.00	23	51.11	3	6.67
	<i>Quercus</i> spp.	43	18	41.86	11	25.58	10	23.26	2	4.65	2	4.65

Fig. 5 Segmented images according to the h value with the highest accuracy

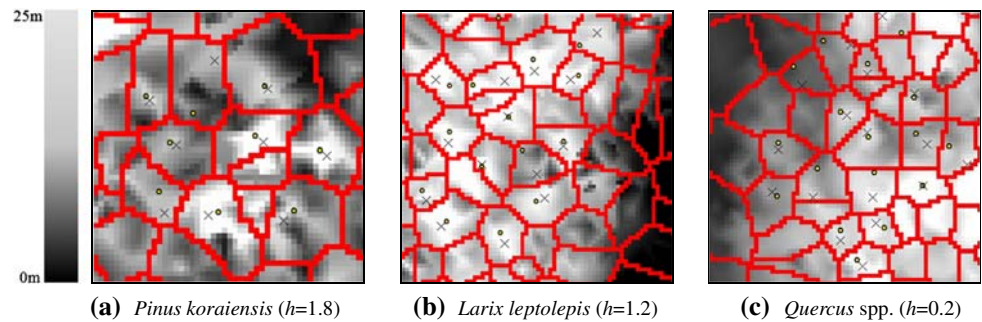
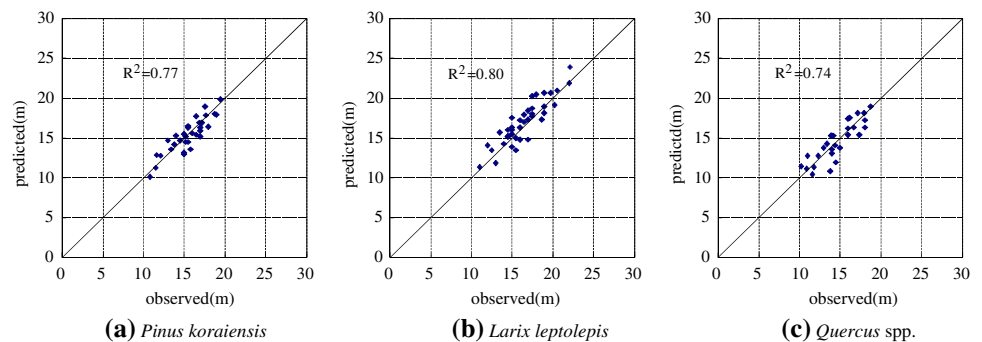


Fig. 6 Accuracies of tree height according to tree species



An average 74.1% of trees in our study were correctly detected although the number of laser points used was relatively small ($1.8 \text{ points m}^{-2}$). This detection accuracy was comparable with that in previous research with higher LiDAR point densities. Heurich et al. (2004) detected 67.9% of trees with 10 points m^{-2} , and Chen et al. (2006) identified 64.1% of trees using $9.5 \text{ points m}^{-2}$. In the study of Koch et al. (2006), the accuracy of the detection was 87.3%, with $5\text{--}10 \text{ points m}^{-2}$, and Solberg et al. (2006) detected 93% of dominant trees with $5.0 \text{ points m}^{-2}$.

However, the main limitation of this study was the low point density of the LiDAR data. Even though the accuracy of this research was comparable with that of previous studies, the DCM cannot accurately describe the shape of an individual tree crown due to the lack of representative LiDAR points with a low point density. Moreover, the laser points used in this work had an across-track average distance of 2.0 m between each line, although the along-track distance was within an average of 1.0 m. The across-track affects the resolution of the DCM, as this depends on the interval between the laser points (Wehr and Lohr 1999). If the point density is higher and the interval of the across-track made sufficiently narrow, a better result can be expected, even if it is not the entire reason for the low accuracy in the detection of trees or estimation of the tree heights.

The problem with the low point density of LiDAR data, as well as low performance, can also affect the accuracy of tree height estimations. The tree height estimations of this study showed relatively low performance compared to the

research of Heurich et al. (2004) with 10 points m^{-2} , in which the coefficients of determination of the tree height estimation were 0.96 and 0.98 for deciduous and coniferous trees, respectively. This can also be attributed to “satisfactory delineation” which could have caused the occurrence of false tree tops in our analysis. With correct delineation, the R^2 for estimating tree heights reached 0.83, 0.86, and 0.78 for *P. koraiensis*, *L. leptolepis*, and *Quercus* spp., respectively. However, the R^2 in satisfactory delineation fell to between 0.25 and 0.58, which causes relatively low statistical performance in tree height estimations (Table 4).

In addition, when LiDAR data are applied for measuring trees and stands in a forest, the DBH–height relationship should be functionalized. Afterward, the DBH can be estimated from the height using LiDAR (Kwak et al. 2005). Trees or stands must also be classified using LiDAR itself (Holmgren and Persson 2004; Koukoulas and Blackburn 2004) or by fusing the digital aerial photograph or satellite imagery with the LiDAR data (Persson et al. 2004; Leckie et al. 2005).

Conclusion

LiDAR data can be effectively used for forest inventory, especially for detecting individual trees and estimating tree heights. This study was performed to delineate individual trees, using the extended maxima transformation of the morphological image-analysis method, and estimate

Table 4 Accuracies of the tree height estimations for correct and satisfactory delineation

	Correct	Satisfactory	Correct and satisfactory
<i>Pinus koraiensis</i>			
Number	25	7	32
R^2	0.83	0.47	0.77
RMSE	1.00	1.35	1.13
<i>Larix leptolepis</i>			
Number	34		39
R^2	0.86	0.25	0.80
RMSE	1.12	2.22	1.35
<i>Quercus</i> spp.			
Number	18	11	29
R^2	0.78	0.58	0.74
RMSE	1.09	1.48	1.32

individual tree heights. For detecting trees and delineating tree crowns, different h values, which play a key role as a factor for controlling the segmentation level, could be applied for different tree species. *P. koraiensis*, *L. leptolepis*, and *Quercus* spp. had best detection accuracies of 68.1% at $h = 0.18$, 86.7% at $h = 0.12$, and 67.4% at $h = 0.02$, respectively. This can be explained by the shape of a deciduous tree crown being rounder than that of a coniferous tree. In other words, a deciduous tree has slightly different elevation values among pixels on the DCM, as it has a gently sloping crown. The coefficients of determination for tree height estimation were 0.77, 0.80, and 0.74 for *P. koraiensis*, *L. leptolepis* and *Quercus* spp., respectively.

The main limitation of this study was the relatively low point density of the LiDAR data. The DCM cannot accurately describe the shape of a crown with a low point density. A low point density can affect the accuracy of detection of individual trees and tree height estimation. Therefore, the point density of LiDAR data needs to be sufficiently improved for better delineation and height estimation of individual trees.

Acknowledgments This work was supported by a Korea Research Foundation Grant funded by the Korean Government (MOEHRD, KRF-2005-213-F00001) and Korea University. Also, we would like to thank Kang-Won Lee for offering the LiDAR data.

References

- Avery TE, Burkhardt HE (1994) Forest measurements, 4th edn. McGraw-Hill, Boston
- Brandtberg T, Walter F (1998) Automated delineation of individual tree crowns in high spatial resolution aerial images by multiple scale analysis. *Machine Vision Appl* 11:64–73
- Brandtberg T, Warner TA, Landenberger RE, McGraw JB (2003) Detection and analysis of individual leaf-off tree crowns in small footprint, high sampling density LiDAR data from eastern deciduous forest in North America. *Remote Sens Environ* 85:290–303
- Chen Q, Baldocchi D, Gong P, Kelly M (2006) Delineating individual trees in a Savanna Woodland using small footprint LiDAR data. *Photogramm Eng Remote Sens* 72:923–932
- Clark ML, Clark DB, Roberts DA (2004) Small-footprint LiDAR estimation of sub-canopy elevation and tree height in a tropical rain forest landscape. *Remote Sens Environ* 91:68–89
- Dougherty ER, Lotufo RA (2003) Hands-on morphological image processing. SPIE, Bellingham
- Dralle K, Rudemo M (1996) Stem number estimation by kernel smoothing of aerial photos. *Can J Forest Res* 26:1228–1236
- Dubayah RO, Drake JB (2000) Lidar remote sensing for forestry. *J Forestry* 98(6):44–46
- Gougeon FA (1995) A crown-following approach to the automatic delineation of individual tree crowns in high spatial resolution aerial images. *Can J Remote Sens* 21:274–284
- Heurich M, Persson Å, Holmgren J, Kennel E (2004) Detecting and measuring individual trees with laser scanning in mixed mountain forest of Central Europe using an algorithm developed for Swedish boreal forest conditions. In: Proceedings of the ISPRS Working Group part 8/2, Int Arch Photogramm Remote Sens vol 36, Freiburg, Germany, October 3–6, 2004, pp 307–312
- Holmgren J, Persson Å (2004) Identifying species of individual trees using airborne laser scanner. *Remote Sens Environ* 90:415–423
- Holmgren J, Nilsson M, Olsson H (2003) Estimation of tree height and stem volume on plots using airborne laser scanning. *Forest Sci* 49:419–428
- Hyypä J, Kelle O, Lehtikoinen M, Inkinen M (2001) A segmentation-based method to retrieve stem volume estimates from 3-D tree height models produced by laser scanners. *IEEE Trans Geosci Remote Sens* 39:969–975
- Koch B, Heyder U, Welnacker H (2006) Detection of individual tree crowns in airborne LiDAR data. *Photogramm Eng Remote Sens* 72:357–363
- Koukoulas S, Blackburn GA (2004) Quantifying the spatial properties of forest canopy gaps using LiDAR imagery and GIS. *Int J Remote Sens* 25:3049–3071
- Kwak DA, Lee WK, Son MH (2005) Application of LiDAR for measuring individual trees and forest stands. *J Korean Forest Soc* 94:431–440
- Kwak DA, Lee WK, Lee JH (2006) Predicting forest stand characteristics with detection of individual tree. In: Proceedings of the MAPP/ASPRS 2006 fall conference, November 6–10, 2006, San Antonio, TX, USA
- Leckie D, Gougeon F, Hill D, Quinn R, Armstrong L, Shreenan R (2003) Combined high-density LiDAR and multispectral imagery for individual tree crown analysis. *Can J Remote Sens* 29:633–649
- Leckie DG, Gougeon FA, Tinis S, Nelson T, Burnett CN, Paradine D (2005) Automated tree recognition in old growth conifer stands with high resolution digital imagery. *Remote Sens Environ* 94:311–326
- Lefsky MA, Harding D, Cohen WB, Parker G, Shugart HH (1999) Surface LiDAR remote sensing of basal area and biomass in deciduous forests of Eastern Maryland, USA. *Remote Sens Environ* 67:83–98
- Lefsky MA, Cohen WB, Parker GG, Harding DJ (2002) Lidar remote sensing for ecosystem studies. *Bioscience* 52:19–30
- Lim K, Treitz P, Groot A, St-Onge B (2001) Estimation of individual tree heights using LIDAR remote sensing. In: Proceedings of the twenty-third annual Canadian symposium on remote sensing, Quebec, QC, Canada, August 20–24, 2001

- Maltamo M, Hyyppä J, Malinen J (2006) A comparative study of the use of laser scanner data and field measurements in the prediction of crown height in boreal forests. *Scand J Forest Res* 21:231–238
- Mei C, Durrieu S (2004) Tree Crown Delineation from digital elevation models and high resolution imagery. In: Proceedings of the ISPRS Working Group part 8/2, Int Arch Photogramm Remote Sens vol 36, Freiburg, Germany, October 3–6, 2004
- Næsset E (1997) Estimating timber volume of forest stands using airborne laser scanner data. *Remote Sens Environ* 61:246–253
- Persson Å, Holmgren J, Söderman U (2002) Detecting and measuring individual trees using an airborne laser scanner. *Photogramm Eng Remote Sens* 68:925–932
- Persson Å, Holmgren J, Söderman U, Olsson H (2004) Tree species classification of individual trees in Sweden by combining high resolution laser data with high resolution near-infrared digital images. In: Proceedings of the ISPRS Working Group part 8/2, Int Arch Photogramm Remote Sens vol 36, Freiburg, Germany, October 3–6, 2004, pp 204–207
- Pollock R (1996) The automatic recognition of individual trees in aerial images of forests based on a synthetic tree crown model. Ph.D. dissertation, Department of Computer Science, University of British Columbia, Vancouver, BC
- Popescu SC, Wynne RH (2004) Seeing the trees in the forest: using lidar and multispectral data fusion with local filtering and variable window size for estimating tree height. *Photogramm Eng Remote Sens* 70:589–604
- Schardt M, Ziegler M, Wimmer A, Wack R, Hyyppä J (2002) Assessment of forest parameters by means of Laser Scanning. In: Proceedings of the IRPRS Commun part 3A, Int Arch Photogramm Remote Sens vol 34, Graz, Austria, September 9–13, 2002, pp 302–309
- Shivers BD, Borders BE (1996) Sampling techniques for forest resource inventory. Wiley, New York
- Soille P (2003) Morphological image analysis: principles and applications, 2nd edn. Springer, Berlin
- Solberg S, Næsset E, Bollandsas OM (2006) Single tree segmentation using airborne laser scanner data in a structurally heterogeneous Spruce forest. *Photogramm Eng Remote Sens* 72:1369–1378
- Wehr A, Lohr U (1999) Airborne laser scanning—an introduction and overview. *ISPRS J Photogramm Remote Sens* 54:68–82
- Wulder MA, Dechka JA, Gillis MA, Luther JE, Hall RJ, Beaudoin A, Franklin SE (2003) Operational mapping of the land cover of the forested area of Canada with Landsat data: EOSD land cover program. *Forestry Chron* 79:1075–1083